Update of $g-2$ of the muon and $\Delta\alpha$

T. Teubner[1] K. Hagiwara[2] R. Liao[1] A.D. Martin[3] Daisuke Nomura[2]

[1] Department of Mathematical Sciences, University of Liverpool, Liverpool L69 3BX, U.K.
[2] Theory Center, KEK, Tsukuba, Ibaraki 305-0801, Japan
[3] Department of Physics and Institute for Particle Physics Phenomenology, University of Durham, Durham DH1 3LE, U.K.

Abstract We update our Standard Model predictions for $g-2$ of the muon and for the hadronic contributions to the running of the QED coupling, $\Delta\alpha^{(5)}_{\rm had}(M_Z^2)$. Particular emphasis is put on recent changes in the hadronic contributions from new data in the 2π channel and from the energy region just below 2 GeV.

Key words Anomalous magnetic moment, muon, running coupling, hadronic contributions

PACS 13.40.Em, 14.60.Ef, 12.15.Lk

1 Introduction

The anomalous magnetic moment of the muon, $a_\mu = (g-2)/2$, has been the subject of wide interest and detailed research. The discrepancy between its experimental value as measured by BNL [1] and its prediction within the Standard Model (SM) is one of the few – if not the only – experimental sign of physics beyond the SM (apart from neutrino mixing). This has triggered a lot of intense scrutiny of both the experimental determination and the theoretical evaluation of a_μ. The BNL experiment E821 has achieved an impressive precision of 0.5ppm [1], and further improvements may only be reached with the planned experiments at Fermilab and J-PARC, see the presentations [2, 3]. As discussed below, the SM prediction relies heavily on the experimental information of the measured hadronic cross sections at low energies. During the last 15 years, the SM prediction has gone through several phases of improvement and consolidation and has now, for the first time, reached an accuracy even slightly better than the experimental value. This is mainly due to the big efforts to measure the hadronic cross sections with increasing accuracy and the progress of various groups working on the data-driven evaluation of the hadronic contributions, which are in fairly good agreement (though further improvements are foreseen as will be discussed briefly in Section 4). In this article we will concentrate on the main changes in the hadronic contributions to a_μ, updating the works [4, 5].

Similarly to $g-2$, the theoretical uncertainties in the running of the QED coupling, $\alpha(q^2)$, are completely dominated by the hadronic contributions, $\Delta\alpha^{(5)}_{\rm had}(q^2)$. Recall $\alpha(M_Z^2)$ is the least well known of the set of precision observables $[G_F, M_Z, \alpha(M_Z^2)]$, so its error is a limiting factor in the electroweak fits of the SM as performed e.g. by the LEP Electroweak Working Group.

2 Standard Model prediction of $g-2$

The anomalous magnetic moment of the muon receives contributions from all sectors of the SM. The QED and electroweak (EW) corrections can be calculated within perturbation theory and are, through many impressive works, well under control. In the compilation for $a_\mu^{\rm SM}$ presented here we use $a_\mu^{\rm QED} = 116584718.08(15)\times 10^{-11}$ [6, 7] and $a_\mu^{\rm EW} = (154\pm 2)\times 10^{-11}$ [8], as e.g. reviewed in Ref. [9]. The hadronic contributions can not be reliably calculated in perturbative QCD (pQCD) as the loop-integrals are dominated by low momentum transfer, i.e. the non-perturbative region of QCD. They are typically divided into the leading (LO) and higher-order (HO) vacuum polarisation (VP), and the so-called light-by-light contributions, which are also subleading: $a_\mu^{\rm had} = a_\mu^{\rm had,\,LO\,VP} + a_\mu^{\rm had,\,HO\,VP} + a_\mu^{\rm had,\,l-by-l}$. While the VP induced corrections can be calculated with methods based on dispersion relations and us-

Received 25 January 2010

1) E-mail: thomas.teubner@liverpool.ac.uk

ing experimentally measured hadronic cross sections as input, the light-by-light scattering contributions can be estimated only using models[1)]. The results from different groups vary considerably, both w.r.t. the mean value and the error. For a review presented at this conference see [10]. In the SM prediction of $g-2$ presented here we use the value $a_\mu^{\mathrm{had,\,l-by-l}} = (10.5 \pm 2.6) \times 10^{-10}$, which has been obtained in [11] as a combination of results based on different models[2)]. In the following we will discuss in more detail recent changes in the VP contributions.

2.1 Hadronic VP contributions

The LO hadronic VP contributions are calculated using the dispersion integral

$$a_\mu^{\mathrm{had,\,LO\,VP}} = \frac{1}{4\pi^3}\int_{m_\pi^2}^{\infty} \mathrm{d}s\, \sigma_{\mathrm{had}}^0(s) K(s)\,, \qquad (1)$$

where $K(s) = \dfrac{m_\mu^2}{3s} \cdot (0.4 \ldots 1)$ is a known kernel function giving highest weight to lowest energies $\sqrt{s}$, and $\sigma_{\mathrm{had}}^0(s)$ is the hadronic cross section for $\mathrm{e^+e^-} \to \gamma^* \to$ hadrons $(+\gamma)$. The superscript ^{0} indicates that the 'undressed' cross section must be used, i.e. the cross section without VP effects in the virtual photon, but including final state radiation (FSR) of photons. To arrive at the best compilation for σ_{had}, at low energies ($\sqrt{s} < 2$ GeV) about 24 hadronic channels (exclusive final states) have to be summed, and in each channel the data from different experiments have to be combined. At intermediate energies σ_{had} is measured inclusively. Perturbative QCD can only be used away from resonances, and (most) data driven analyses use pQCD only for energies above the open $\mathrm{b\bar{b}}$ threshold. For details of the data input, their treatment w.r.t. radiative corrections and the data combination through a non-linear χ^2_{min} fit, as used in the work reported here, see Refs. [4, 5]. Note that there are uncertainties w.r.t. the correct application of radiative corrections (undressing of VP, possible addition of neglected photon FSR) to the data, especially in the case of older data sets. In our analysis this leads to the assignment of a separate error due to radiative corrections, $\delta a_\mu^{\mathrm{had,\,VP+FSR}} \simeq 1.8 \cdot 10^{-10}$, which alone is about ten times bigger than the uncertainty of the electroweak contributions a_μ^{EW}.

2.1.1 Recent changes in the 2π channel

More than 70% of a_μ^{had} is coming from the $\rho \to 2\pi$ channel. Following older experiments, the cross section $\mathrm{e^+e^-} \to \pi^+\pi^-$ has been measured in recent years with increasing accuracy by the Novosibirsk experiments CMD-2 and SND, see e.g. Ref. [14] for a short review of their results. Fig. 1 displays the impressive agreement of the most recent data sets from CMD-2 and SND, together with recent data from KLOE [15] obtained with the method of Radiative Return (see [16] for a detailed review of the method and its application, and [17] for the very new KLOE analysis of the 2π channel presented at the PhiPsi09 conference but not yet available for public use). The grey band shows the result of our data combination in this channel including also older data, but excluding the KLOE data, see the discussion below.

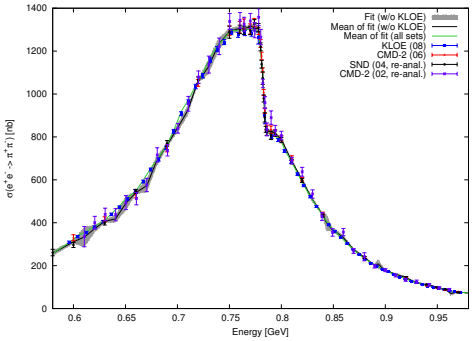

Fig. 1. (color online) Most important data in the 2π channel and fits as described in the text.

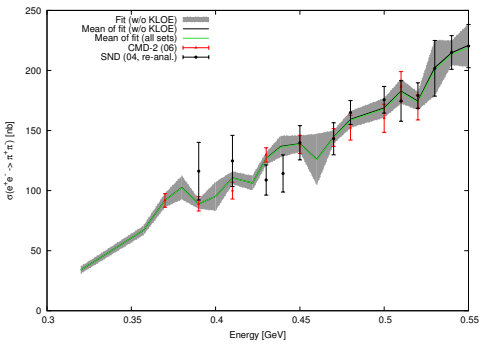

Fig. 2. Low energy region close to the 2π threshold.

The lowest energy region close to the 2π threshold is displayed in Fig. 2. The recent CMD-2 data represented by (red) triangles and error bars clearly demonstrate the improvement from this single data set alone, with the fit in this region being dominated by these data. Fig. 3 shows an enlargement of the ρ-ω interference region which is now very well mapped out by the consistent data sets. However, Fig. 3 also

1) First principle calculations within lattice gauge field theory are underway but very difficult and at an early stage.

2) Note that this is slightly different from (though certainly compatible with) the value $a_\mu^{\mathrm{had,\,l-by-l}} = (116 \pm 40) \times 10^{-11}$ as obtained in Refs. [12, 13] and discussed in Ref. [10].

shows that the KLOE data are undershooting the combination of the other data in this region, while typically being higher than other data at lower energies as can be seen by the (green) solid line in Fig. 1. This apparent difference in shape is highlighted in Fig. 4, which shows the normalised difference of the KLOE cross section and the combination of the other 2π data by the square markers, while the band displays the size of the error of the compilation without KLOE. (The bands displayed in the figures are obtained from the diagonal elements of the fit's full covariance matrix.)

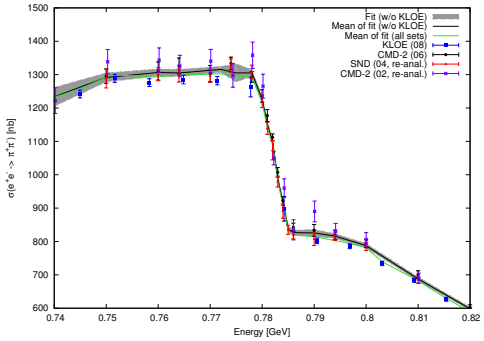

Fig. 3. ρ-ω interference region in the 2π channel.

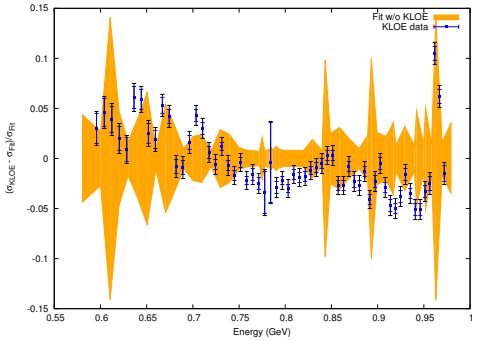

Fig. 4. Normalised difference of the KLOE data [15] and the data compilation excluding KLOE; the band represents the error of the compilation.

One should keep in mind that the KLOE data are obtained via the method of Radiative Return at fixed collider centre-of-mass energy, whereas the other data are measured via the traditional method of energy scan by adjusting the e^+e^- beam energies. Hence Monte Carlo simulation tools including radiative corrections and also the systematic effects are completely different between the two approaches. Up to now it is not clear what causes the difference in the shapes of the 2π data, and more studies are underway to clarify the situation. Unfortunately this difference in shape prevents us from including the KLOE data in a straightforward way in the non-linear $\chi^2_{\rm min}$ fit[1)]. Note that if we calculate the contribution to $g-2$ from the KLOE data alone, we obtain $a_\mu^{\pi\pi,\,\rm KLOE} = (384.16 \pm 3.47) \times 10^{-10}$, in perfect agreement with the result of the integral over our compilation of all 2π data without KLOE (but in the range of the KLOE data), for which we get $a_\mu^{\pi\pi,\,\rm w/out\ KLOE} = (384.12 \pm 2.51) \times 10^{-10}$. We therefore use the procedure adopted already in [4] where earlier KLOE data (now superseded by [15]) were included after integration, by calculating a weighted average with the integral over the data compilation without KLOE, and not performing a point-by-point combination.

BaBar has also published their first measurement of the 2π channel based on Radiative Return [18] (see also [19]), finding some discrepancies with KLOE. We have not included the new BaBar data in the analysis presented here as they were not available for public use at the time of the conference, but see [20, 21] for an analysis which includes them.

2.1.2 Energy region below 2 GeV

Important changes in the data input have also happened in the region between 1.4 and 2 GeV. This region is particularly difficult, as a growing number of multi-hadron exclusive final states becomes accessible and has to be included to obtain $\sigma_{\rm had}$ with good accuracy. However, these energies are above the reach of the Novosibirsk machine[2)], and the quality of the available data was not very good. Alternatively, one can rely on inclusive R measurements, but for this only rather old and not very precise data are available. This situation has changed with BaBar measuring, through Radiative Return, many channels with higher accuracy than earlier experiments. These include new data for $2\pi^+2\pi^-$ [23], $K^+K^-\pi^0$, $K^0_S\pi K$ [24], $2\pi^+2\pi^-\pi^0$, $K^+K^-\pi^+\pi^-\pi^0$, $2\pi^+2\pi^-\eta$ [25], $2\pi^+2\pi^-2\pi^0$ [26] used for our updated analysis. Figs. 5 – 7 exemplify the influence of the new BaBar data. The new data are not always in good agreement with other sets; in such cases the fit has a poor quality and we scale up the error of the channel's contribution by $\sqrt{\chi^2_{\rm min}/\text{d.o.f.}}$ (e.g. in the $2\pi^+2\pi^-2\pi^0$ channel $\chi^2_{\rm min}/\text{d.o.f.} = 2.7$.)

1) The fit allows a readjustment of the overall normalisation of the data sets within their systematic errors. Including the KLOE data would lead to a bad $\chi^2_{\rm min}$/d.o.f. and unnatural normalisation effects pulling the fit upward, see [4] for a detailed discussion.

2) This will change with the current upgrade, see [22].

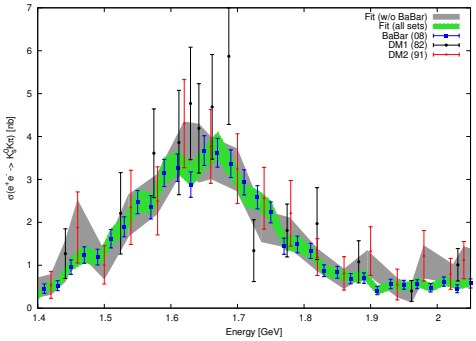

Fig. 5. $K^0_S K\pi$ channel with improvement due to recent BaBar data [24].

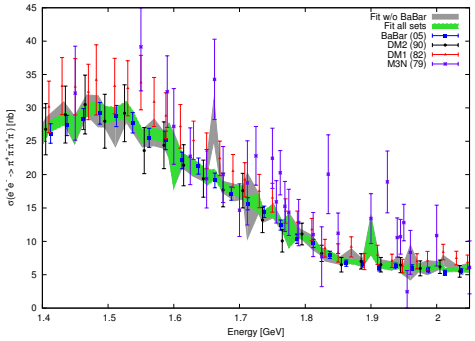

Fig. 6. $2\pi^+2\pi^-$ channel.

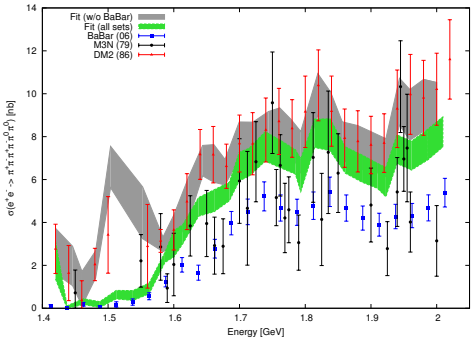

Fig. 7. $2\pi^+2\pi^-2\pi^0$ channel.

2.1.3 Sum rule analysis

Note that in previous $g-2$ analyses [4, 5] we found a discrepancy between using the available inclusive data in the region 1.4 to 2 GeV and adding the exclusive channels. The inclusive data were lower than the sum of the exclusive channels, though they were found to be similar in shape.

In [5] we performed a QCD sum rule analysis, concluding that the inclusive data are more compatible with pQCD and the world average of α_s, and therefore chose to use the inclusive data instead of the sum over the exclusive for energies $\sqrt{s} = 1.43\ldots2$ GeV. Since then the situation has changed: the hadronic data has changed slightly, being lower at low energies and also at energies above 2 GeV. Also, with the inclusion of the recent BaBar data the sum of the exclusive channels in the region 1.4 to 2 GeV has become slightly lower and more accurate than before. Our updated sum rule analysis is summarised in Fig. 8; different sum rules based on pQCD are made to match the corresponding sum rule integrals over the data by fitting for α_s as a free parameter (see [5] for details). It is clear that the new sum over exclusive channels is more accurate than the old inclusive data and also more compatible with the predictions based on pQCD with a world average value of α_s. We therefore are now combining the results from the inclusive and the sum over exclusive data in this energy region[1)].

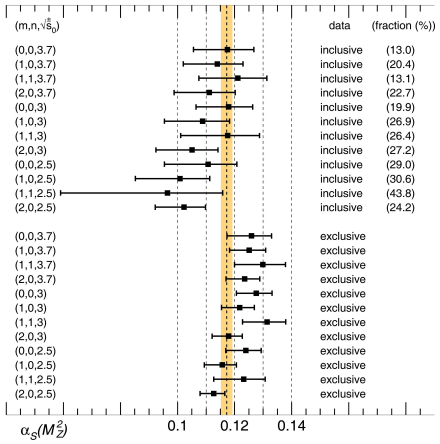

Fig. 8. Results for different sum-rules [5] translated into a prediction of α_s; the band shows the world average of $\alpha_s(M_Z^2)$.

2.1.4 Other changes and result for $a_\mu^{\mathrm{had,\,VP}}$

In addition to the important changes discussed above, compared to [4], we have also included new data in other channels: K^+K^- from CMD-2 [27] and SND [28], $K^0_S K^0_L$ from SND [29], $\pi^+\pi^-\pi^0$ from CMD-2 [30], $\omega\pi^0$ from KLOE [31], and inclusive R data at higher energies above 2 GeV from BES [32, 33] and CLEO [34]. Fig. 9 shows the recent BES data together with the fit of all inclusive data in this region and the prediction from pQCD. While the contribution to $g-2$ is significantly smaller than previously, it is obvious that pQCD, which is in perfect agreement with the three latest BESII (09) data points [33], is still somewhat lower than the fit for energies below 3 GeV.

1) Note that the sum over exclusive channels stills requires, due to the lack of experimental information, the use of iso-spin relations for unknown channels, which in turn results in a large error from the poorly known $K\bar{K}\pi\pi$ channel.

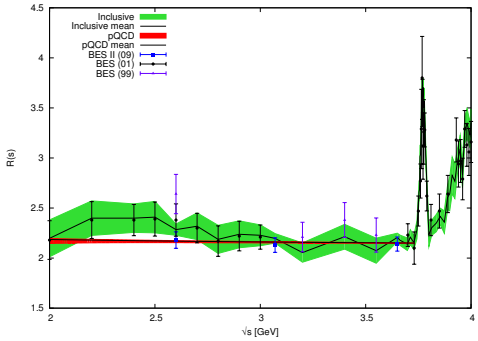

Fig. 9. Recent data from BES together with the fit of all inclusive data compared to pQCD in the energy region above 2 GeV.

Numerically the changes to $a_\mu^{\mathrm{had,\,LO\,VP}}$ from the different energy regions amount to (units of 10^{-10}, compared to results from [4]): -0.76 (0.32–1.43 GeV, low energy exclusive channels), $+2.10$ (1.43–2 GeV, results from inclusive and sum over exclusive data combined), -1.35 (2 – 11.09 GeV, higher energy inclusive data). This accidentally leads to a near perfect cancellation of the shifts, with the total result $a_\mu^{\mathrm{had,\,LO\,VP}} = (689.4 \pm 3.6_{\mathrm{exp}} \pm 1.8_{\mathrm{rad}}) \times 10^{-10}$. The first error is coming from the statistical and systematic error of the data, whereas the second error is our estimate of the uncertainty in the radiative corrections as mentioned above. However, compared to our earlier result from [4], $a_\mu^{\mathrm{had,\,LO\,VP}}(\mathrm{HMNT06}) = (689.4 \pm 4.2_{\mathrm{exp}} \pm 1.8_{\mathrm{rad}}) \times 10^{-10}$, there is a further reduction in the error.

The higher-order VP induced contributions can also be calculated using a dispersion integral, see [5] for details. Our updated result is nearly unchanged and reads $a_\mu^{\mathrm{had,\,HO\,VP}} = (-9.79 \pm 0.06_{\mathrm{exp}} \pm 0.03_{\mathrm{rad}}) \times 10^{-10}$.

2.2 SM predictions compared to the BNL measurement

Combining the QED, EW and hadronic contributions as discussed above, we arrive at our SM prediction of the anomalous magnetic moment of the muon,

$$a_\mu^{\mathrm{SM}}(\mathrm{HLMNT09}) = (116\ 591\ 773 \pm 48) \times 10^{-11}. \quad (2)$$

Due to a small shift of Codata's muon to proton magnetic ratio λ the experimental value for a_μ from BNL is now $a_\mu^{\mathrm{EXP}} = 116\ 592\ 089(63) \times 10^{-11}$ [2]. This results in a difference $a_\mu^{\mathrm{EXP}} - a_\mu^{\mathrm{SM}} = (31.6 \pm 7.9) \times 10^{-10}$ which corresponds to a $4\,\sigma$ discrepancy. The situation is displayed in Fig. 10 where we also show our previous result and the most recent results from Jegerlehner and Nyffeler [13] and three different predictions from Davier et al. [20, 21, 35]: While their e^+e^- based result without the new BaBar 2π (labelled 'w/o BaBar (09)' in the figure) data agrees very well with our evaluation, the result including these new data lead to a shift upwards, but still compatible with the other e^+e^- based result. The third result employs, in addition to e^+e^- data, also the use of τ spectral function data from ALEPH, OPAL, CLEO and BELLE.

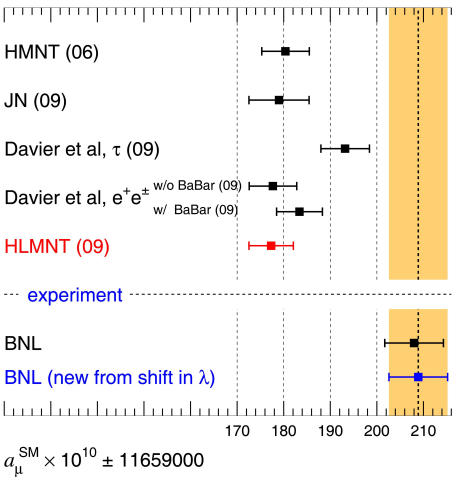

Fig. 10. Comparison of recent predictions for $g-2$ compared to the BNL measurement.

To translate the charged current induced hadronic τ decay data into the required spectral functions requires the application of isospin breaking corrections, which can only be predicted in a model dependent way. Earlier τ based results from Davier et al. were incompatible with e^+e^- based results, but with a re-evaluation of the isospin breaking corrections [21, 35, 36] they find the result displayed in Fig. 10 (labelled 'τ (09)') which is now marginally consistent. These findings were discussed controversially at the PhiPsi09 conference; Benayoun presented an alternative approach based on Hidden Local Symmetry and dynamical (ρ, ω, ϕ) mixing. With this and with a global fit he gets consistency of the τ spectral function with the e^+e^- data and an improved 2π contribution to $g-2$ [37]. Keeping in mind that other studies obtained a very large uncertainty of the isospin breaking corrections (see e.g. Ref. [38]) we believe that, until this issue is better understood, the predictions of $g-2$ based on e^+e^- data alone are more reliable.

3 Running QED coupling $\alpha(q^2)$

Based on the same data compilation, we also predict the hadronic contributions to the running of the QED coupling, $\alpha(q^2) = \alpha/(1 - \Delta\alpha_{\mathrm{lep}} - \Delta\alpha_{\mathrm{had}})$. The

hadronic VP is important for many studies where high accuracy radiative corrections are required, as is the case for the hadronic contributions to $g-2$, see [16] for a very recent review. Of particular importance as input in EW precision fits is the quantity $\Delta\alpha^{(5)}_{\rm had}(M_{\rm Z}^2)$, the hadronic contributions to the running α from five-flavours (the contribution from the top quark is usually added using pQCD). Our updated value is $\Delta\alpha^{(5)}_{\rm had}(M_{\rm Z}^2) = 0.02760 \pm 0.00015$. This is slightly higher and significantly more accurate than the number from Burkhardt and Pietrzyk used as default by the LEP EW Working Group, and leads e.g. to a lower preferred Higgs mass and a lower upper limit from the famous 'Blue Band Plot'.

4 Summary and outlook

We have given an update of the SM prediction of $g-2$, emphasising recent developments for the hadronic contributions. With the e^+e^- based analysis presented here we obtain a $4\,\sigma$ discrepancy between the experimentally measured value of a_μ and its SM prediction. Slightly less significant discrepancies are reported by other groups, depending on the data used and the details of the analyses. However, for all e^+e^- based analyses the discrepancy is about $3-4\,\sigma$ and standing all scrutiny.

For the future, further improvements of the SM prediction will be possible. The method of Radiative Return has proven extremely powerful and will be leading to many more results. In addition to the already reported new 2π data from KLOE [17], further analyses are ongoing, and there are exciting prospects with KLOE2 [39]. There is also a rich programme going on at BELLE, and the possibility of SuperBELLE at the horizon. CMD-3 and SND at VEPP-2000 currently commissioned in Novosibirsk are aiming at largely improving the exclusive measurements in the region below 2 GeV, whereas BESIII at BEPCII will cover higher energies. With all these developments the error of the SM prediction of $g-2$ is expected to shrink even further, so that in the future the light-by-light contributions may eventually become the limiting factor. Obviously there is an extremely strong case for new the $g-2$ experiments as planned by the $g-2$ Collaboration for Fermilab [2] and at J-PARC [3]. With this, $g-2$ will become even more powerful in establishing and constraining physics beyond the Standard Model.

References

1 Bennett G W et al. Phys. Rev. D, 2006, **73**: 072003
2 Roberts L. These proceedings
3 Mibe T. These proceedings
4 Hagiwara K et al. Phys. Lett. B, 2007, **649**: 173
5 Hagiwara K et al. Phys. Rev. D, 2004, **69**: 093003
6 Kinoshita T, Nio M. Phys. Rev. D, 2006, **73**: 053007
7 Aoyama T et al. Phys. Rev. D, 2008, **77**: 053012
8 Czarnecki A, Marciano W J, Vainshtein A. Phys. Rev. D, 2003, **67**: 073006; 2006, **73**: 119901
9 Passera M. These proceedings
10 Nyffeler A. These proceedings
11 Prades J, de Rafael E, Vainshtein A. arXiv:0901.0306
12 Nyffeler A. Phys. Rev. D, 2009, **79**: 073012
13 Jegerlehner F, Nyffeler A. Phys. Rept., 2009, **477**: 1
14 Ignatov F for the CMD-2 and SND Collaborations. Nucl. Phys. Proc. Suppl., 2008, **181-182**: 101
15 KLOE Collaboration, Ambrosino F et al. Phys. Lett. B, 2008, **670**: 285
16 Actis S et al. arXiv:0912.0749
17 KLOE Collaboration, presented by Stefan E. Müller. These proceedings, arXiv:0912.2205
18 BaBar Collaboration, Aubert B et al. Phys. Rev. Lett., 2009, **103**: 231801
19 Wang W. These proceedings
20 Davier M et al. arXiv:0908.4300
21 Davier M. These proceedings, arXiv:1001.2243
22 Tikhonov Yu. These proceedings
23 BaBar collaboration, Aubert B et al. Phys. Rev. D, 2005, **71**: 052001
24 BaBar collaboration, Aubert B et al. Phys. Rev. D, 2008, **77**: 092002
25 BaBar collaboration, Aubert B et al. Phys. Rev. D, 2007, **76**: 092005
26 BaBar collaboration, Aubert B et al. Phys. Rev. D, 2006, **73**: 052003
27 CMD-2 collaboration, Akhmetshin R R et al. Phys. Lett. B, 2008, **669**: 217
28 SND collaboration, Achasov M N et al. Phys. Rev. D, 2007, **76**: 072012
29 SND collaboration, Achasov M N et al. J. Exp. Theor. Phys., 2006, **103**: 720
30 CMD-2 collaboration, Akhmetshin R R et al. Phys. Lett. B, 2007, **642**: 203
31 KLOE collaboration, Ambrosino F et al. Phys. Lett. B, 2008, **669**: 223
32 BES collaboration, Ablikim M et al. Phys. Rev. Lett., 2006, **97**: 262001
33 BES collaboration, Ablikim M et al. Phys. Lett. B, 2009, **677**: 239
34 CLEO collaboration, Besson D et al. Phys. Rev. D, 2007, **76**: 072008
35 Davier M et al. arXiv:0906.5443
36 Lopez Castro G. These proceedings
37 Benayoun M. These proceedings
38 Melnikov K, Vainshtein A. Theory of the Muon Anomalous Magnetic Moment. Berlin: Springer, 2006. (Chapter 3.6)
39 Venanzoni G. These proceedings